Involvement of DNA sensors in different types of skin injury

Čuljak, Klara

Master's thesis / Diplomski rad

2021

Degree Grantor / Ustanova koja je dodijelila akademski / stručni stupanj: **University of Zagreb, Faculty of Food Technology and Biotechnology / Sveučilište u Zagrebu, Prehrambeno-biotehnološki fakultet**

Permanent link / Trajna poveznica: https://urn.nsk.hr/urn:nbn:hr:159:257347

Rights / Prava: Attribution-NoDerivatives 4.0 International/Imenovanje-Bez prerada 4.0 međunarodna

Download date / Datum preuzimanja: **2025-02-20**

UNIVERSITY OF ZAGREB

FACULTY OF FOOD TECHNOLOGY AND BIOTECHNOLOGY

MASTER THESIS

Université d'Orléans - Université de Zagreb

UFR Sciences et Techniques- Faculté de Nutrition et Biotechnologie -
Faculté des Sciences

Master Sciences du Vivant

Spécialité : Biotechnologies, Biologie Moléculaire et Cellulaire

INTERNSHIP REPORT

Involvement of DNA sensors in different types of skin injury

Klara Čuljak

(February, 2021 – July, 2021)

Internship institution and address: Immunologie Neurogénétique Expérimentales et Moléculaires, UMR7355 INEM, 3B rue Ferollerie, 45100 Orléans, Group "Immune responses to infections and pollutants"

Supervisor: Bernhard Ryffel, scientist, M.D., Ph.D.

Zagreb, September 2021

ABSTRACT

Skin, the first organ in contact with the environment, plays an important role in protection against pathogens, chemical, mechanical and other injuries. However, superficial skin injuries can disrupt the integrity of the skin and thus lead to the development of numerous diseases that are nowadays widely present. As the concentration of pollutants in the air increases over the years, various skin injuries occur more and more often. Some of the most destructive air pollutants are ozone, ultraviolet radiation, cigarette smoke, particular matter, and many others. According to previous studies, these pollutants are very harmful to human lungs. To determine whether such substances have the same effect on the skin, we established four research models – tape strip injury as a mechanical damage model, acute and chronic ozone, and cigarette smoke exposure as models of chemical damage. According to histological analyses and levels of inflammatory mediators, we found that mechanical damage of the skin is more destructive than chemical one. Also, IFNAR, NLRP3 and STING showed to be promising targets for future research as they revealed a possible protective role in skin injury.

RÉSUMÉ

La peau, premier organe en contact avec l'environnement, joue un rôle important dans la protection contre les agents pathogènes, les produits chimiques, les traumatismes mécaniques. Cependant, les lésions cutanées superficielles peuvent perturber l'intégrité de la peau et ainsi conduire au développement de nombreuses maladies qui sont aujourd'hui largement présentes. À mesure que la concentration de polluants dans l'air augmente au fil des ans, diverses lésions cutanées surviennent de plus en plus fréquemment. Certains des polluants atmosphériques les plus destructeurs sont l'ozone, les rayons ultraviolets, la fumée de cigarette, des matières particulières et bien d'autres. Selon des études antérieures, ces polluants sont très nocifs pour les poumons humains. Pour déterminer si de telles substances ont le même effet sur la peau, nous avons établi quatre modèles de recherche: les blessures par bandes adhésives comme modèle de dommages mécaniques, l'exposition aiguë et chronique à l'ozone et à la fumée de cigarette comme modèles de dommages chimiques. Selon les analyses histologiques et les niveaux de médiateurs inflammatoires, nous avons constaté que les dommages mécaniques de la peau sont plus destructeurs que les dommages chimiques. En outre, IFNAR, NLRP3 et STING se sont révélés être des cibles prometteuses pour de futures recherches car ils ont révélé un rôle protecteur possible dans les lésions cutanées.

Mots-clés: fumée de cigarette, capteurs d'ADN, ozone, lésions cutanées, lésions des bandes adhésives

SAŽETAK

Koža kao zaštitni organ u svih živih organizama, prva dolazi u doticaj s različitim utjecajima iz okoliša poput patogena, kemijskih, mehaničkih i drugih ozljeda. Površinske ozljede kože mogu utjecati na integritet kože i uzrokovati razvoj brojnih bolesti široko rasprostranjenih u svijetu. Onečišćenje zraka povećava se s godinama i utječe na sve češću pojavu ozljeda kože. Najveći onečišćivači zraka poput ultraljubičastog zračenje, dima cigareta, ozona i mnogih drugih prema brojnim istraživanjima imaju negativan učinak na dišni sustav. Cilj rada bio je utvrditi imaju li navedeni zagađivači i negativan utjecaj na kožu. Uspostavljena su četiri modela istraživanja: mehanička ozljeda kože (ozljeda kože ljepljivom trakom) i kemijska ozljeda kože (akutno izlaganje ozonu, kronično izlaganje ozonu te izlaganje dimu cigareta). Histološkom analizom i mjerenjem razina upalnih medijatora utvrdili smo da je mehaničko oštećenje kože destruktivnije u odnosu na kemijsko oštećenje. DNA senzori IFNAR, NLRP3 i STING pokazali su najveći potencijal u zacjeljivanju kože nakon ozljede. S obzirom na kratko razdoblje istraživanja, navedene DNA senzore i njihovu zaštitnu ulogu treba opsežnije istražiti u budućnosti.

Ključne riječi: dim cigareta, DNA senzori, ozljeda kože, ozljeda ljepljivom trakom, ozon

PRESENTATION OF THE LABORATORY

The experimental part of this master thesis project has taken place at the laboratory of Experimental and Molecular Immunology and Neurogenetics, UMR7355 INEM (fr. *Immunologie et Neurogénétique Expérimentales et Moléculaires*) located in Orléans, France within the group "Immune responses to infections and pollutants".

Laboratory of Experimental and Molecular Immunology and Neurogenetics (INEM) is a research unit of the French National Centre for Scientific Research, CNRS, (fr. *Le Centre national de la recherche scientifique*) and in its work, it is also affiliated with the University of Orléans in France. The scientific objectives of UMR7355 INEM are to study molecular and cellular mechanisms involved in host-pathogen relationships, pulmonary inflammation, genetics of autism and mental disabilities, and neurotoxicity processes during development. Also, researches are based on analysis of the mechanisms involved in certain pathologies which would further allow to identify and validate molecular targets of interest. INEM is a laboratory that works with the industry which provides the access to cutting-edge reagents and it created a start-up in 2010, Artimmune, in order to transfer service contracts. They have double competence and complex integrated models which allow to understand pathophysiological mechanisms in immunology/inflammation and neuropathology, and also try to develop a transversal project in neuroinflammation by the different teams. Six different teams make up the basic organizational structure of the INEM laboratory: Immune responses to infections and pollutants, Inflammation, danger signals, infection, and pulmonary pathologies, Neurogenetics, Neurotoxicity and Development, Artimmune and Laboratory Commun Artinem.

During the internship, my part of the research was done within the group "Immune responses to infections and pollutants" led by Valérie Quesniaux. The team's scientific objective is to focus on understanding the host's response to infections, at the molecular and cellular levels. As dysfunction of the immune system can lead to reactivation of infections, they are studying the role of certain cytokines such as tumor necrosis factor (TNF) or interleukin 1 (IL-1) in control of these responses using genetically modified mice.

Table of contents

List of tables

Table of figures

1. INTRODUCTION

1.1. Skin – roles and structure

Skin is the largest organ of the human body and it has multiple key roles required for interacting with the environment. One of its most significant functions is to prevent and protect the human body from environmental hazards such as ultraviolet (UV) radiation, physical and chemical insults, and microorganisms, and to prevent loss of endogenous substances. Also, skin regulates temperature, prevents dehydration, and has self-healing properties (Honari *et al.*, 2017).

The structure of skin is organized in the 3 main layers: epidermis, dermis, and hypodermis. The epidermis is an outermost layer that has a major role as a barrier function, protection from UV and it acts as a spot for activating innate immunity. Its thickness is 0,05 - 1 mm depending on which part of the body it is located. The epidermis is mostly composed of keratinocytes, melanocytes, and Langerhans cells. Keratinocytes are the predominant cells that are constantly generated in the basal lamina and go through maturation, differentiation, and migration to the surface. During keratinocyte differentiation 3 layers are formed above the basal layer in the following order: stratum spinosum, stratum granulosum, and stratum corneum (SC) (Figure 1) (Honari *et al.*, 2017). The stratum corneum is mostly composed of free fatty acids, ceramides, and esterols and it consists of non-viable keratinocytes, known as corneocytes. Corneocytes are embedded in the intracellular lipid membranes (Bouwstra and Honeywell-Nguyen, 2002).

The dermis represents an integrated system of fibrous cellular and acellular matrix composed of numerous cells such as fibroblasts, masts cells, macrophages, and circulating immune cells. It is loaded with blood vessels and nerves and it is extremely important for skin flexibility, elasticity, and tensile strength. The dermis has a major role in protecting against mechanical damage of the skin as well as wound healing as it contains and supports receptors for sensory stimuli (Honari *et al.*, 2017).

The hypodermis is the deepest and the thickest skin layer mostly composed of adipose tissue as well as connective tissue, larger nerves, blood vessels, and macrophages. Its role is temperature regulation, energy storing, and attaching the upper skin layers (Honari *et al.*, 2017).
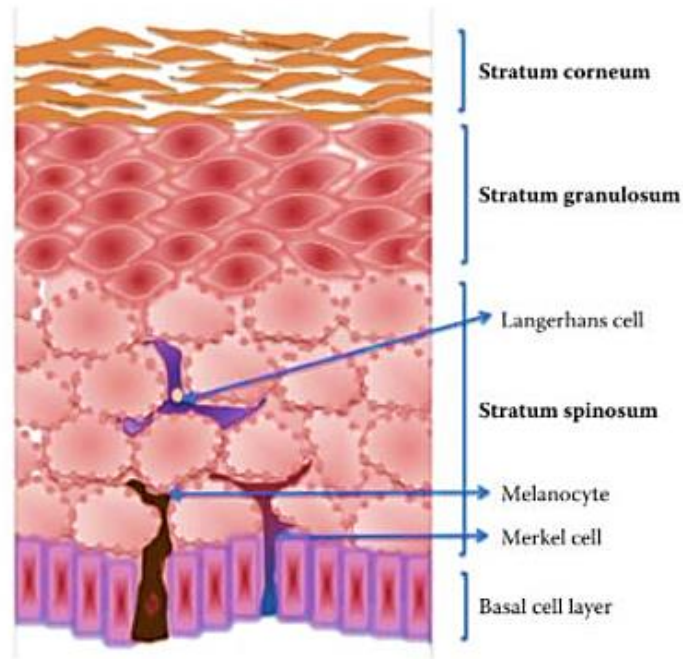
Figure 1. Structure of epidermis: stratum spinosum, stratum granulosum, stratum corneum (Honari et al., 2017).

1.2. Skin injury

One of the world's major health problems is non-healing skin wounds. In a healthy person, any skin damage activates a well-controlled inflammatory and tissue repair response. These responses lead to pathogen removal and wound healing. However, in non-healing wounds, these processes are either missing or overactive leading to abnormal tissue formation or a long-lasting defect of the epidermis barrier (Di Domizio *et al.*, 2020). The most common skin diseases are psoriasis (characterized by scaly, red cutaneous plaques), allergic contact dermatitis, atopic dermatitis (exaggerated cutaneous immune response to environmental antigens), hives, and acne (Robert and Kupper, 1999).

There are two types of skin injuries based on the source of damage: mechanical and chemical.

1.2.1. Mechanical damage of skin

Mechanical damage of the skin involves the movement of the epidermal layer, more precisely stratum corneum, which leads to inflammatory processes. One of the methods for mechanical skin damage, which was also used in this research, is tape strip injury.

1.2.2. Chemical damage of skin

On the other hand, chemical damage of the skin represents air pollutants such as ultraviolet radiation (UV), polycyclic aromatic hydrocarbons (PAH), cigarette smoke (CS), ozone (O_3), oxides, particular matter (PMs), and volatile organic compounds (VOCs). They affect the outermost skin barrier by inducing oxidative stress and inflammation, thus stimulating the production of pro-inflammatory cytokines. As a consequence, skin aging occurs, as well as the appearance of inflammatory and allergic skin conditions such as psoriasis, acne, eczema, and in extreme cases, skin cancer (Drakakiet *et al.,* 2014). Prolonged or repetitive exposure to high levels of pollutants may have negative effects on the skin even though skin acts as a biological shield.

1.2.2.1. Ozone

Ozone (O_3) is one of the most toxic air pollutants and the main component of photochemical smog. High concentrations of ozone are found in the stratosphere and such ozone has a positive effect as it absorbs UV light coming from the Sun. Thusly, such ozone protects the Earth from dangerous rays. On the other hand, tropospheric ozone molecules are formed by the interaction of UV light and hydrocarbons and nitrogen oxides which are emitted by automobile tailpipes and smokestacks. These kinds of molecules are both, harmful to human health as air pollutants and greenhouse gases, trapping heat and contributing to climate change (Logan, 1985).

In addition to the harmful effects of ozone as an air pollutant, ozone also has positive effects that are widely exploited in the cosmetics industry. Namely, ozone is recognized as one of the best bactericidal, antiviral and antifungal agents. It is used as a clinical therapeutic agent for chronic wounds and various ulcers helping to heal and reduce bacterial infections. However, if ozone is used in excessive concentrations for those purposes it can have profound negative effects (Kim *et al.*, 2009).

The first target of ozone on the skin is the stratum corneum which contains numerous unsaturated fatty acids and lipids. Namely, ozone does not penetrate directly into the skin. First, it reacts with lipids thus generating bioactive molecules such as free radicals (ROS – reactive oxygen species), lipid peroxidation products (such as 4-hydroxynonenal), and oxidation of functional groups. Hence, it leads to the alteration of membrane permeability and induction of inflammatory responses (Ferrara *et al.*, 2019). Ozone stimulates the production of matrix metalloproteinases (MMPs) that are responsible for the degradation of extracellular components such as elastin and collagen, implicated in extrinsic skin aging (Drakaki *et al.*, 2014).
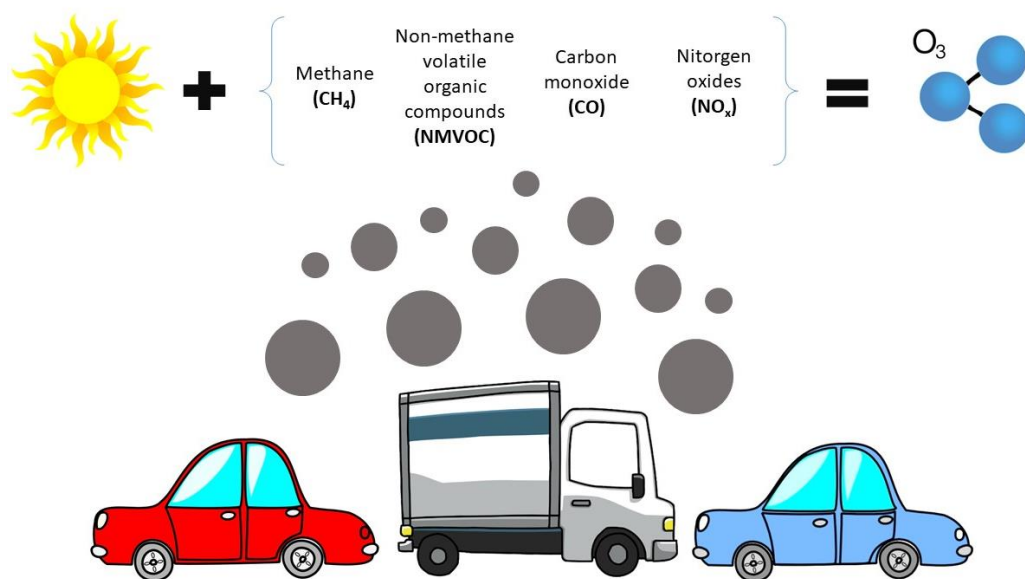
Figure 2. Simplified scheme of tropospheric ozone formation

1.2.2.2.Cigarette smoke

Cigarette smoke is a very complex aerosol consisting of a thousand molecules such as reactive nitrogen and oxygen species and electrophilic aldehydes. Many of these species are highly carcinogenic, tumor promoters, or cocarcinogenic. Free radicals from cigarette smoke cause oxidative stress and lipid peroxidation of the skin. Those processes disrupt membrane permeability and integrity which then cause accelerated skin aging. Chemical components of cigarette smoke activate transepidermal water loss, degeneration of connective tissue, an increase of matrix metalloproteinases MMP-1, MMP-3, and MMP-9, and decreased wound healing capacity (Drakaki *et al.*, 2014).

1.3. Mechanisms involved in wound healing

After skin damage, the healing process takes place in three overlapping phases: the inflammatory phase, the proliferative phase, and tissue remodeling. Numerous cytokines, chemokines, and growth factors resulting from active innate immunity are required to heal and regenerate the skin after injury. Various studies have shown that inflammasome is active after a skin injury and that it greatly contributes to accelerated skin repair after an injury. Therefore, one of the main factors for fast, well-controlled, and successful skin repair is the stage of inflammation (Hattori *et al.*, 2019).

One group of the cytokines that plays an important role in initiating the inflammatory response are type I interferons (INF), a family of antiviral cytokines comprising 13 IFN-α and one IFN-

β. The inflammatory response is stimulated by the activation of T cells and dendritic cells. In wound repair, a subset of dendritic cells (DC) called plasmacytoid dendritic cells (pDC) have a major role in type I IFN production. Type I IFN expression in skin wounds occurs *via* activation of TLR9 which suggests that pDC can recognize extracellular DNA fragments released in the context of injury (Di Domizio *et al.*, 2020). Recent studies suggest that innate sensing of DNA in pDC is not limited only to endosomes but that it can also occur *via* cytosolic receptors in a TLR9 independent manner (Benmerzoug *et al.*, 2019).

1.3.1. cGAS / STING pathway

The cGAS / STING pathway has a potential role in wound repair by activating a gene encoding type I interferon expression. cGAS is a cytoplasmic DNA-sensor cyclic GMP-AMP synthase which after DNA recognition and its oligomerization produces an endogenous second messenger cyclic GMP-AMP (cGAMP). cGAMP binds to the endoplasmic reticulum protein, stimulator of interferon genes STING, and thus traffics together to the endoplasmic reticulum (ER), Golgi intermediate compartment (ERGIC), and Golgi apparatus. Here, activated STING subsequently recruits tank-binding kinase 1 (TBK1) leading to the activation of IFN regulatory factor 3 (IRF3) by its phosphorylation. Activated IRF3 dimerizes and translocates to the nucleus inducing type I IFNs and other proinflammatory cytokines (Benmerzoug *et al.*, 2019; Hattori et al., 2019) (Figure 3).

1.3.2. INF signaling mediated by JAK/STAT pathway

The IFNs and IFN-like molecules lead to activation of JAK/STAT signaling pathway. Namely, the binding of interferons to their heterodimeric transmembrane IFNα receptor (IFNAR) leads to conformational changes and activation of the janus activated kinase (JAK) family of tyrosine kinases. These kinases selectively phosphorylate signal transducers and transcription activators (STATs), leading to their activation. Activated STATs separate from receptors, dimerize, and translocate to the nucleus where they induce the expression of the INF and other target genes (Kisseleva *et al*., 2002; Pestka *et al*., 2004; Ivashkiv and Donlin, 2014).

1.3.3. NLRP3 signaling pathway

The innate immune system is the first line of host defense in which germline-encoded pattern-recognition receptors (PRRs) have a major role in response to harmful stimuli, cellular damage or environmental irritants. An inflammasome is defined by its sensor protein (a PRR), which then oligomerizes and forms a pro-caspase-1 activating platform in response to damage-associated molecular patterns (DAMPs) or pathogen-associated molecular patterns (PAMPs). NLRP3 (leucine-rich repeat (LRR)-containing proteins (NLR) family member) is one of the

five members of PRRs which can form inflammasomes. Once activated, it potently modulates innate immune function by regulating the maturation and secretion of pro-inflammatory cytokines such as IL1β and IL18 (Tschopp and Schroder, 2010).
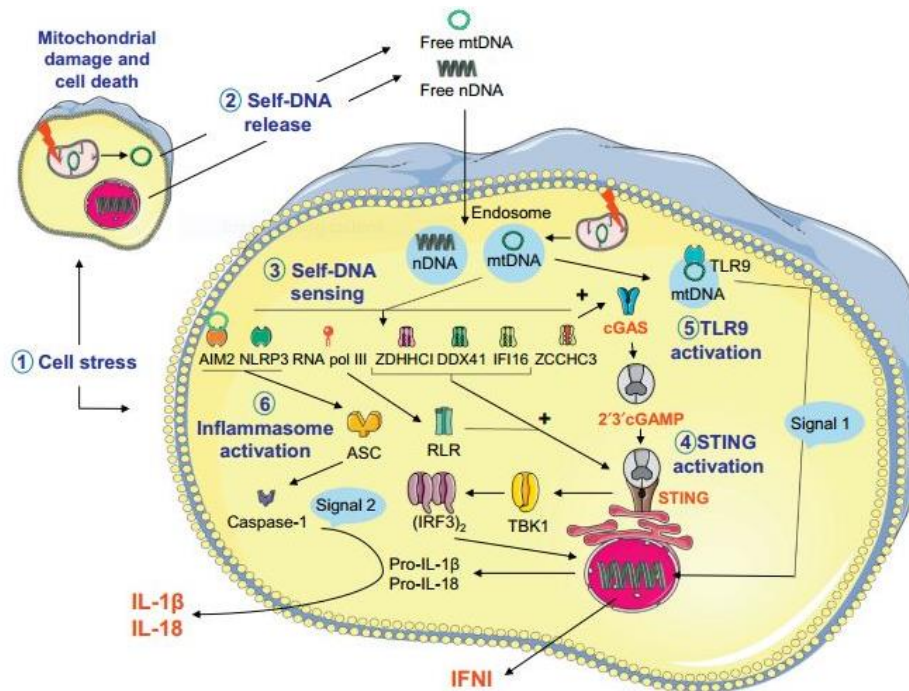
Figure 3. Nucleic acid sensing in different cellular compartments (Benmerzoug et al., 2019).

1.4. Objectives

In this project, four different models of skin injury were used – tape strip injury as a mechanical model; acute and chronic ozone exposure and cigarette smoke exposure as chemical models. The main objective of this study was to investigate whether host-derived DNA released upon epithelial mechanical or chemical damage contributes to wound repair through DNA sensing cGAS-STING- type I IFN pathway activation as well as through activation of other DNA sensors such as IFNAR and NLRP3.

2. MATERIALS AND METHODS

2.1. Mouse models and their treatment

Both knock-out and wild-type mice listed below were bred and housed at UPS44-TAAM (CNRS, Orléans, France) temperature-controlled (23 °C) animal facility and they were given free access to food and water.

2.1.1. Tape strip injury model (TSI)

Mouse models used for the experiments were 11- to 12-week-old female and male mice of four different genotypes: wild-type (C57BL/6J; WT) and knock-out mice *(Cgas$^{-/-}$, Sting$^{-/-}$, Ifnar$^{-/-}$)*. Tape strip injury was performed by pulling duct tape over the back of both ears of the anesthetized mouse around 20 times. For each wild-type and knock-out mouse group, there was a control group of mice (air group) on which no tape strip injury was performed. The mice were then measured for body weight and their ear exterior was observed over the next four days. Ear exterior was described according to the three different parameters: ear thickness, erythema, and scaling. Parameters were evaluated as described in Tables 1 and 2. The cumulative value of all three parameters was obtained and used in further analyses. On the fourth day, mice were euthanized by progressive CO_2 inhalation and necropsy was performed in which one ear was taken for protein extraction and ELISA, and the other ear for histology.

Table 1. Correlation between score values and ear thickness

Score	Ear thicknes (mm)
0	<24
1	25-35
2	36-45
3	46-55
4	56-65
5	>66

Table 2. Correlation between score values and erythema and scaling of the ear skin

Score	0	1	2	3
Erythema	no redness	mild redness	medium redness	severe redness
Scaling	no peeling skin	mild peeling skin	medium peeling skin	severe peeling skin

2.1.2. Acute ozone model

Mouse models used for the experiments were 6- to 11-week-old female and male mice of four different genotypes: wild-type (C57BL/6J; WT) and knock-out mice *(Cgas^{-/-}, Sting^{-/-}, Ifnar^{-/-}, Nlrp3^{-/-})*. Mice were exposed to ozone in a plexiglass chamber (EMB 104, EMMS®) at 1,5 ppm for one hour. Ozone was created by an ozonisator (Ozonisator Ozoniser S 500mg, Sander®) and the level of 1,5 ppm was controlled by a sensor (ATI 2-wire transmitter, Analytical Technology®). For each wild-type and knock-out mouse group, there was a control group of mice (air group) that was not exposed to ozone. Mice were euthanized by progressive CO_2 inhalation 24 hours after ozone exposure and necropsy were performed in which one ear was taken for protein extraction and ELISA, and the other ear for histology.

2.1.3. Chronic ozone model

Mouse models used for the experiments were 8- to 11-week-old female mice of three different genotypes: wild-type (C57BL/6J; WT) and knock-out mice *(Sting^{-/-} and Nlrp6^{-/-})*. Mice were exposed to ozone in a plexiglass chamber (EMB 104, EMMS®) at 0,5 – 1,5 ppm in a duration time from 30 minutes to two hours during six weeks according to Figure 4. Ozone was created by an ozonisator (Ozonisator Ozoniser S 500mg, Sander®) and the level of ozone was controlled by a sensor (ATI 2-wire transmitter, Analytical Technology®). For each wild-type and knock-out mouse group, there was a control group of mice (air group) that was not exposed to ozone. Mice were euthanized by progressive CO_2 inhalation 24 hours after last ozone exposure and necropsy were performed in which one ear was taken for protein extraction and ELISA, and the other ear for histology.
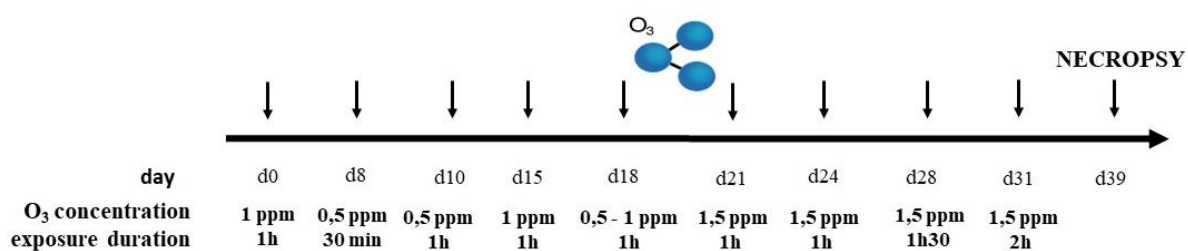

Figure 4. Plan of chronic ozone exposure of the mice

2.1.4. Cigarette smoke model (CS)

Mouse models used for the experiments were 8- to 11-week-old female and male mice of three different genotypes: wild-type (C57BL/6J; WT) and knock-out mice *(Gsdmd$^{-/-}$ and Nlrp3$^{-/-}$)*. Exposure of mice to cigarette smoke was performed using a calibrated EMKA InExpose smoking robot. Mice were exposed to cigarette smoke three times per day for four cigarettes for 20 min in a whole-body chamber for four days. For those purposes 3R4F research cigarettes (University of Kentucky) were used with the filter removed and the cigarettes were puffed once per minute, 4 s duration, 200 ml puff volume. Following this exposure, wild-type (C57BL/6J; WT) and knock-out *(Gsdmd$^{-/-}$, Nlrp3$^{-/-}$)* mice were subjected to cigarette smoke as described above, while control groups for each knock-out and wild-type mouse (air group) were not exposed to cigarette smoke. On the fifth day, mice were euthanized by progressive CO_2 inhalation and necropsy was performed in which one ear was taken for protein extraction and ELISA, and the other ear for histology.

2.2. Tissue preparation and hematoxylin and eosin staining (HE)

Dissected ears which were previously stored in 4% paraformaldehyde, were embedded in paraffin. Tissue blocks were used for preparing 3 μm thick tissue sections by microtome (Leica) which were further used for HE staining. First, the tissue sections were deparaffinised in xylene for ten minutes and then rehydrated in 100%, 95%, and 75% alcohol baths for one minute for each bath. Afterward, the thus deparaffinised and rehydrated samples were stained first in Gill's hematoxylin bath for staining the nuclei for three minutes and then in an eosin bath for staining the cytoplasm for one minute. Before Gill's hematoxylin staining and after eosin staining, the samples were left in distilled water for one minute, while between stainings, the samples were washed in tap water to remove stain residues. In the end, dehydration of the tissues was performed by bathing the samples in 75%, 95%, and 100% alcohol baths during ten seconds for each, and then transferring in xylene bath for ten minutes. Subsequently, samples were mounted with a mounting medium (Eukit$^{®}$) and scanned by NanoZoomer.

2.3. Protein extraction and protein dosage

Ears previously-stored at -80 °C which were taken for protein level analyses, were used for protein extraction by sonication. Protein extraction was performed in Tissue Protein Extraction Reagent (Invitrogen) containing a Halt^{TM} protease and phosphatase inhibitor cocktail (1/100, Invitrogen). After the sonication, the crude protein extracts were centrifuged at 10000 rpm for ten minutes. Protein concentrations were measured by Pierce^{TM} BCA Protein Assay Kit

(Thermo Fisher) following manufacturer's instructions. Absorbance was measured at 562 nm by ELX800 Microplate reader (Fisher Scientific).

2.4. ELISA dosage

The obtained protein extracts were used for cytokine levels measurement by ELISA. Murine myeloperoxidase (MPO), lipocalin-2 (LCN2), tumor necrosis factor alpha (TNFα), matrix metalloproteinase-9 (MMP9), and interleukin-6 (IL6) levels were analysed by ELISA Assay Kits (DuoSet®, R&D Systems) according to manufacturer's instructions. Absorbance was measured at 450 nm by ELX800 Microplate reader (Fisher Scientific).

2.5. Statistical analysis

All the data were analysed by GraphPad Prism (GraphPad Software Inc., San Diego, CA, USA; www.graphpad.com). The Mann-Whitney non-parametric test was performed and all the values are expressed in the form of mean ± SEM. Statistical significance was defined at a *p*-value *** < 0.001, ** < 0.01, and * < 0.05. Statistical differences between the experimental groups were represented by a star on the top of the column.

3. RESULTS

3.1. Mechanical damage of the skin – tape strip injury

3.1.1. Ear exterior and histological analyses

To examine whether inflammation occurred after performing tape strip injury, the thickness of the ears was measured as well as a clinical score value over four days. The clinical score value is defined as a cumulative value of three parameters: ear thickness, erythema, and scaling.

Tape strip injury induced an increase in the ear thickness in wild-type, $Cgas^{-/-}$ and $Sting^{-/-}$ groups of mice, while $Ifnar^{-/-}$ group of mice showed almost constant ear thickness values over the course of four days. The ear thickness of the control groups of mice (air groups) remained the same over four days (Figure 5).
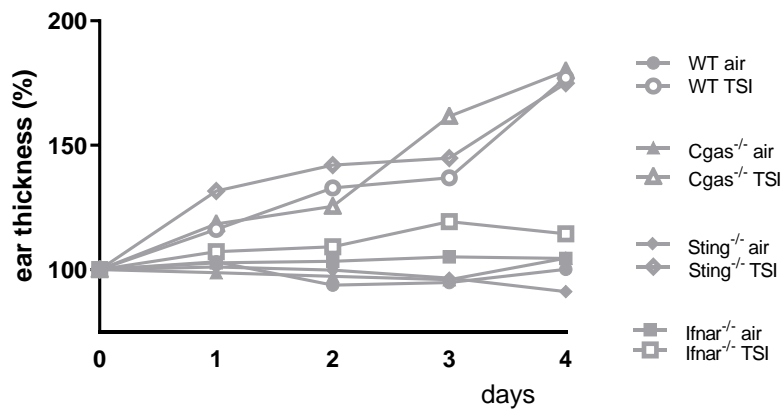
Figure 5. Ear thickness over four days after performing tape strip injury on a wild-type, $Cgas^{-/-}$, $Sting^{-/-}$ and $Ifnar^{-/-}$ groups of mice.

All TSI groups of mice showed high clinical score values, while the highest values were detected for the $Cgas^{-/-}$ TSI group. Clinical score values of the control groups of mice (air groups) remained the same over four days (Figure 6).
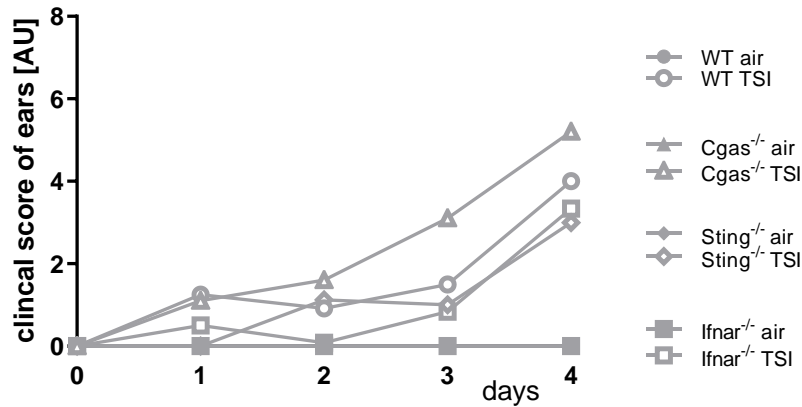
Figure 6. Clinical score values over four days after performing tape strip injury on a wild-type, *Cgas$^{-/-}$, Sting$^{-/-}$* and *Ifnar$^{-/-}$* groups of mice.

To determine whether there was cellular infiltration and inflammation, HE staining of ear tissue sections was performed. Cellular infiltration and inflammation occurred in wild-type and Cgas knock-out TSI groups of mice comparing to matching control groups (air groups) (Figure 7b, 7d). Cellular infiltration was indicated by the increase in the thickness of the outer layer of the epidermis, stratum corneum, and a number of cells in the deeper layers of the epidermis (Figure 7, indicated with arrows). On the other hand, an increase in the ear thickness was not found in *Ifnar$^{-/-}$* group of mice and partially in the *Sting$^{-/-}$* group of mice (Figure 7f, 7h).
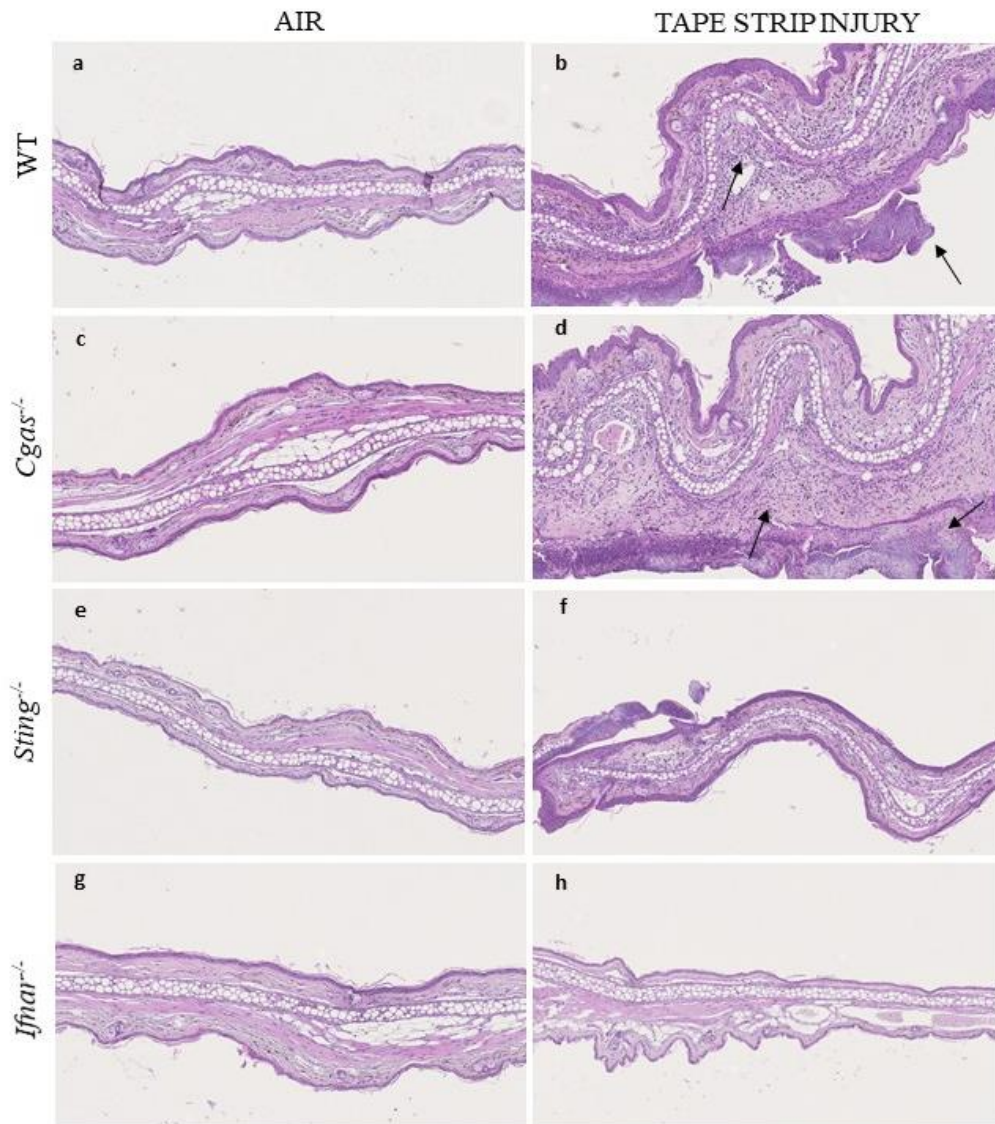
Figure 7. Histological evaluation and comparison of hematoxylin and eosin stained ears of control groups of mice (air groups) (a, c, e, g) and tape strip injury groups of mice (b, d, f, h) for both wild-type (WT) and knock-out mice (*Cgas^{-/-}, Sting^{-/-}, Ifnar^{-/-}*). Photos were taken under 10x of magnification.

3.1.2. Protein dosage and inflammatory mediator production

The occurrence of protein leakage was detected by measuring the concentration of total proteins. Namely, no significant difference was observed in the concentration of total proteins comparing all control groups (air groups) and TSI groups of both, wild-type and knock-out mice (Figure 8).

Figure 8. Protein concentration after performing tape strip injury on a wild-type, $Cgas^{-/-}$, $Sting^{-/-}$ and $Ifnar^{-/-}$ groups of mice. Data are represented as mean ± SEM. *** P < 0.001, ** P< 0.01, and * P< 0.05.

Lastly, to observe whether inflammation occurred, levels of MPO, LCN2, MMP9, and IL6 were detected by ELISA. MPO production increased significantly in the $Cgas^{-/-}$ TSI group of mice compared to the matching control group ($Cgas^{-/-}$ air) (Figure 9a). No significant difference in LCN2, MMP9, and IL6 production between TSIs and matching control groups were detected (Figure 9b-d). Reduced production of cytokines MPO, LCN2, and MMP9 was observed for the $Ifnar^{-/-}$ TSI groups of mice in comparison to wild-type TSI groups, while for the cytokine IL6 there was no difference (Figure 9a-c).
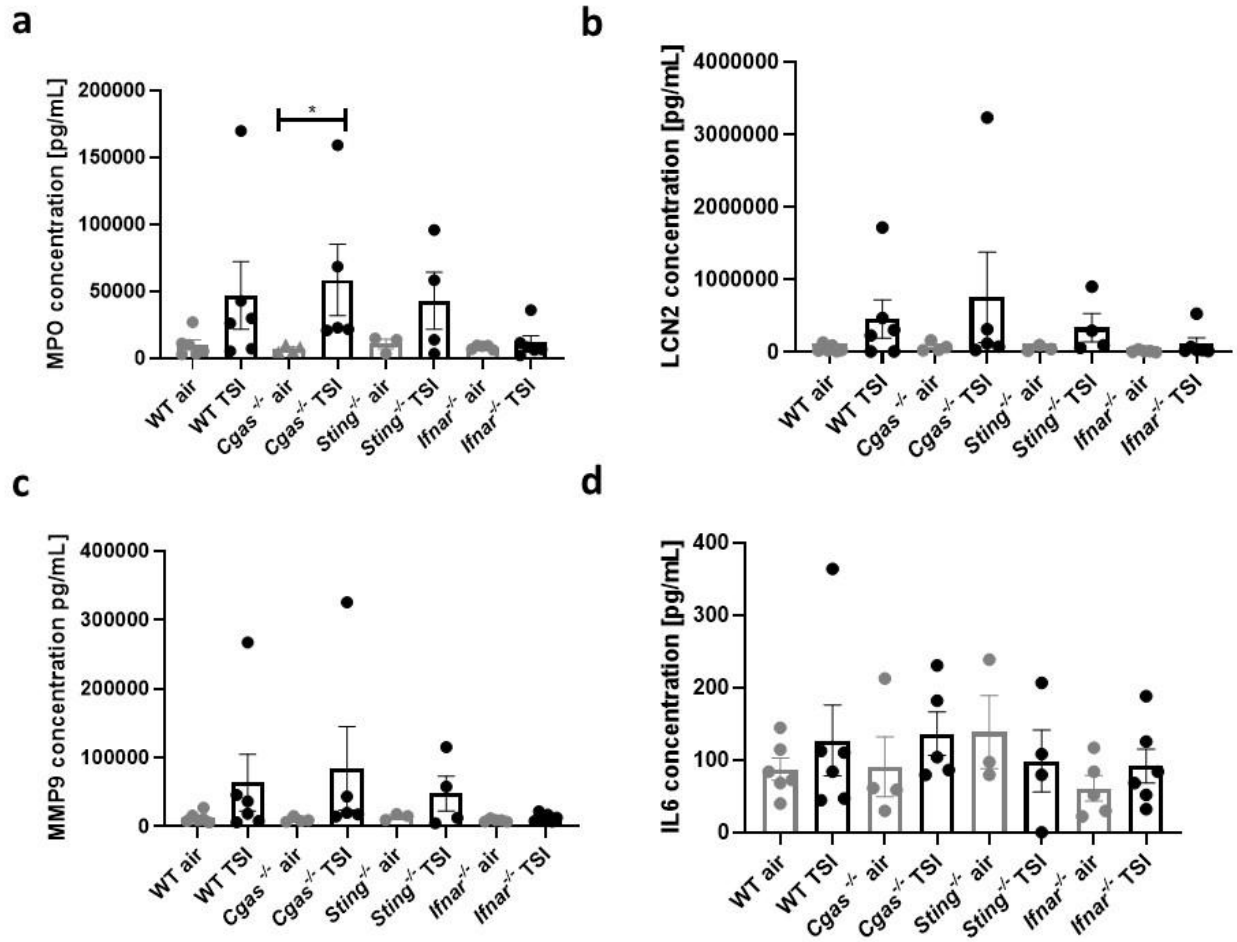
Figure 9. MPO (a), LCN2 (b), MMP9 (c) and IL6 (d) concentration after performing tape strip injury on a wild-type, *Cgas$^{-/-}$*, *Sting$^{-/-}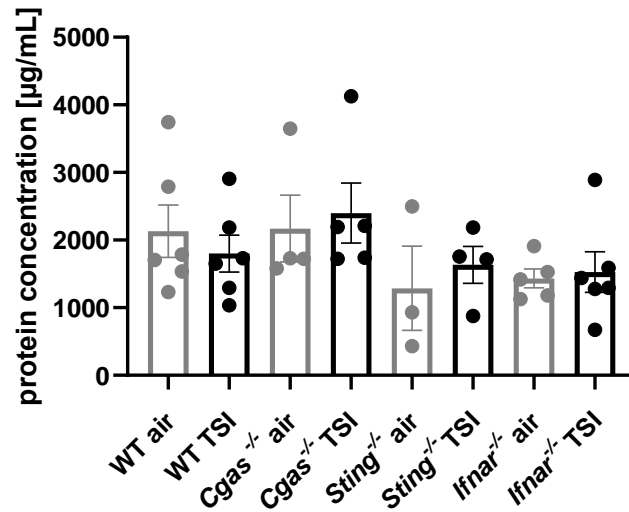$* and *Ifnar$^{-/-}$* groups of mice. Data are represented as mean ± SEM. *** $P < 0.001$, ** $P < 0.01$, and * $P < 0.05$.

3.2. Chemical damage of the skin – acute ozone model

3.2.1. Histological analysis

Histological analysis of ear tissue sections from the mice that were subjected to acute ozone exposure did not show any differences comparing to matching control groups (air groups). No inflammation or cellular infiltration was detected in neither acute ozone groups or genotypes according to histological examination. Also, no difference in the ear thickness was observed (Figure 10).

Figure 10. Histological evaluation and comparison of hematoxylin and eosin stained ears of control groups of mice (air groups) (a, c, e, g, i) and groups of mice which were subjected to acute ozone exposure (1,5 ppm, during 1 hour) (b, d, f, h, j) for both wild-type (WT) and knock-out mice ($Cgas^{-/-}$, $Sting^{-/-}$, $Ifnar^{-/-}$, $Nlrp3^{-/-}$). Photos were taken under 20x of magnification.

3.2.2. Protein dosage and inflammatory mediator production

Firstly, the level of total proteins was measured in order to examine whether there was increased protein leakage due to ozone exposure. No significant difference was observed in the concentration of total proteins comparing all control (air groups) and ozone groups of both, wild-type (WT) and knock-out ($Cgas^{-/-}$, $Sting^{-/-}$, $Ifnar^{-/-}$, $Nlrp3^{-/-}$) mice (Figure 11).

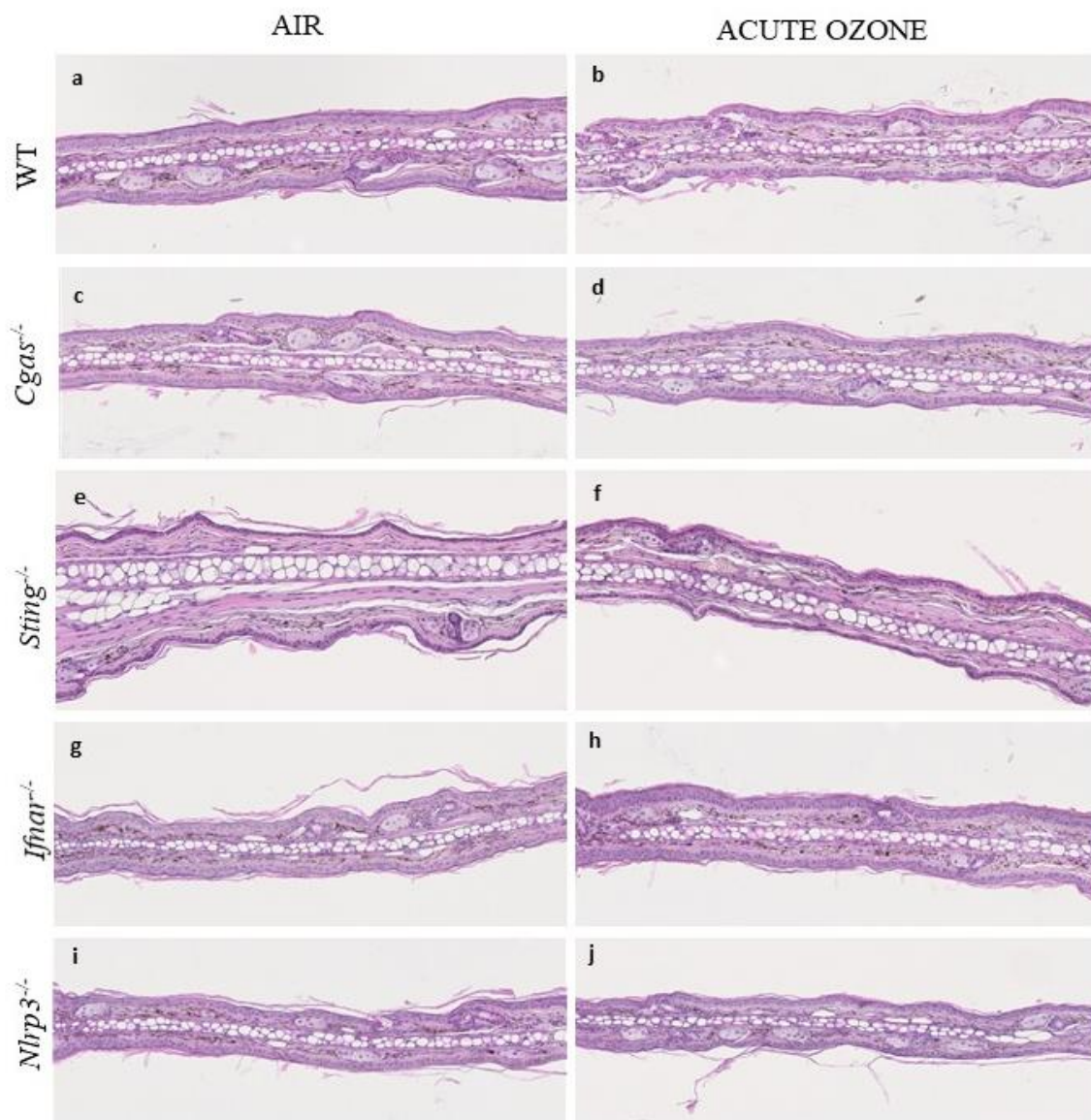*Figure 11*. Protein concentration after acute ozone exposure (1,5 ppm, during 1 hour) of wild-type (WT) and knock-out ($Cgas^{-/-}$, $Sting^{-/-}$, $Ifnar^{-/-}$, $Nlrp3^{-/-}$) groups of mice. Data are represented as mean ± SEM. *** P < 0.001, ** P< 0.01, and * P< 0.05.

Secondly, levels of four inflammatory mediators, MPO, LCN2, MMP9, and IL6, were measured in order to detect whether inflammation occurred. LCN2 and IL6 production increased significantly in WT ozone groups of mice compared to matching control groups (WT air) (Figure 12b, 12d). No significant difference in MPO and MMP9 production was observed comparing ozone groups of mice with matching control groups (air groups) (Figure 12a, 12c). On the other hand, $Ifnar^{-/-}$ and $Nlrp3^{-/-}$ ozone groups of mice showed lower production of the cytokine LCN2 in comparison to the wild-type ozone groups of mice (Figure 12b). The same trend was detected in the production of the cytokine IL6, but in addition to the above, reduced production was also observed in the $Sting^{-/-}$ ozone group of mice (Figure 12d).
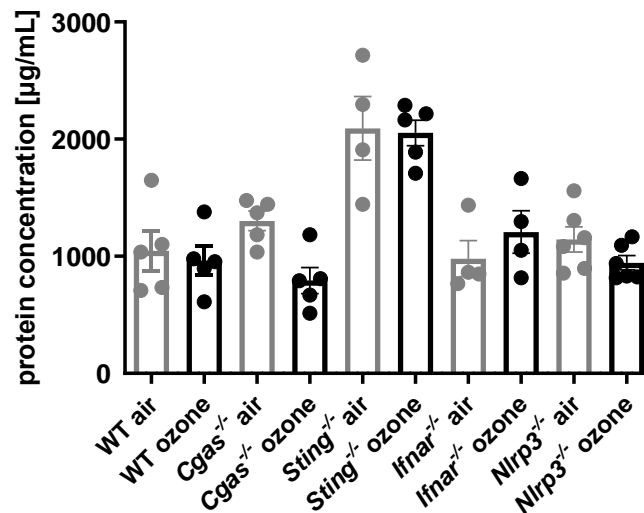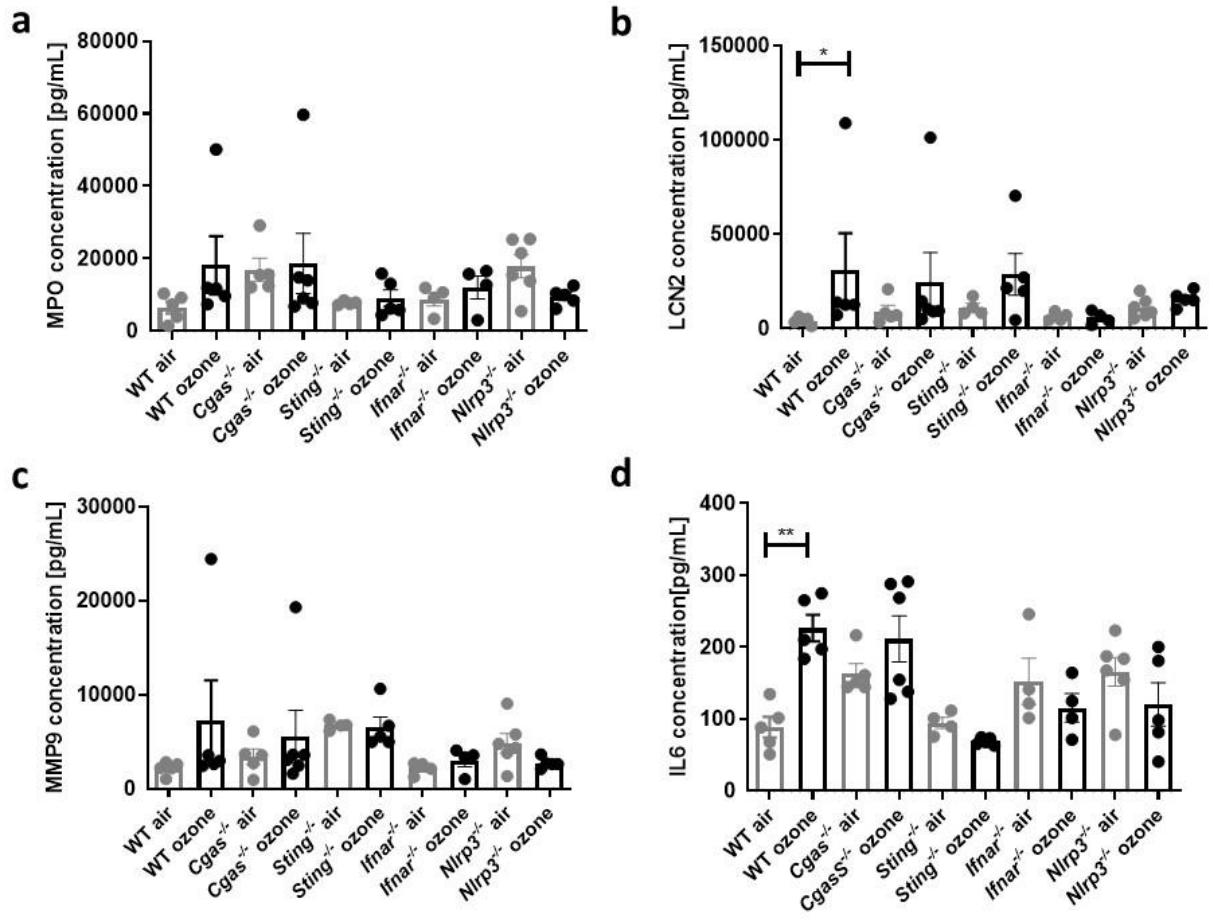
Figure 12. MPO (a), LCN2 (b), MMP9 (c) and IL6 (d) concentration after acute ozone exposure (1,5 ppm, during 1 hour) of wild-type (WT) and knock-out (*Cgas*^{-/-}, *Sting*^{-/-}, *Ifnar*^{-/-}, *Nlrp3*^{-/-}) groups of mice. Data are represented as mean ± SEM. [***] P < 0.001, [**] P < 0.01, and [*] P < 0.05.

18

3.3. Chemical damage of the skin – chronic ozone model

3.3.1. Histological analysis

Histological evaluation of ear tissue sections from the mice that were subjected to chronic ozone exposure indicated no inflammation, cellular infiltration, or difference in ear thickness between chronic ozone groups of mice and matching control groups (Figure 13).
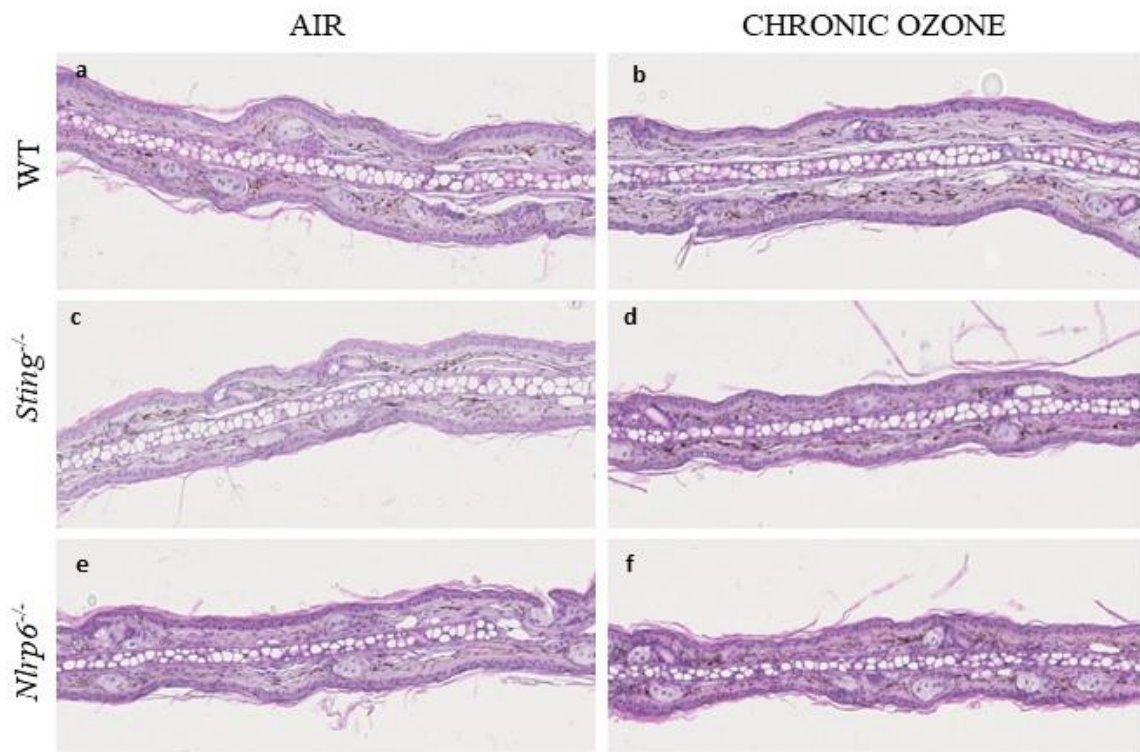
Figure 13. Histological evaluation and comparison of hematoxylin and eosin stained ears of control groups (air groups) of mice (a, c, e) and groups of mice which were subjected to chronic ozone exposure (0,5-1,5 ppm, 2 times per week, during 6 weeks) (b, d, f) for both wild-type (WT) and knock-out mice (*Sting-/-, Nlrp6-/-*). Photos were taken under 20x of magnification.

3.3.2. Protein dosage and inflammatory mediator production

In order to detect whether inflammation occurred, the concentration of total proteins was measured. No significant difference was observed in the concentration of total proteins comparing all control groups (air groups) and ozone groups of both, wild-type (WT) and knock-out (*Sting-/-, Nlrp6-/-*) mice (Figure 14).

Figure 14. Protein concentration after chronic ozone exposure (0,5-1,5 ppm, 2 times per week, during 6 weeks) of wild-type (WT) and knock-out (*Sting*^{-/-}, *Nlrp6*^{-/-}) groups of mice. Data are represented as mean ± SEM. [***] $P < 0.001$, [**] $P < 0.01$, and [*] $P < 0.05$.

For detecting changes in the production of inflammatory mediators, levels of four cytokines MPO, LCN2, MMP9, and IL6 were measured by ELISA. IL6 production decreased significantly in the *Sting*^{-/-} ozone group of mice compared to matching control (*Sting*^{-/-} air) (Figure 15d). On the other hand, MPO, LCN2, and MMP9 production did not show any significant difference between ozone groups of mice and matching control groups (air groups) (Figure 15a-c).

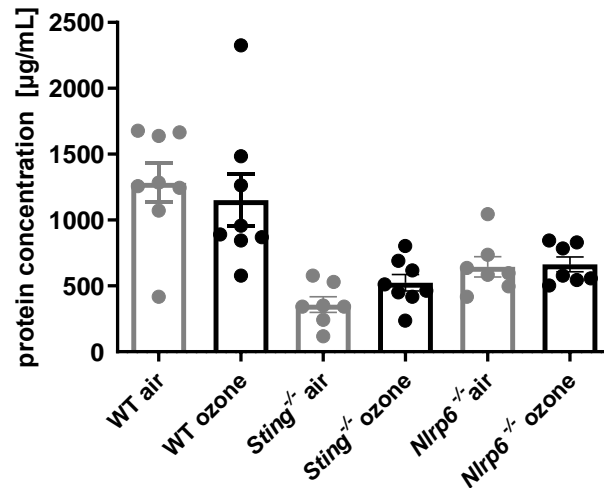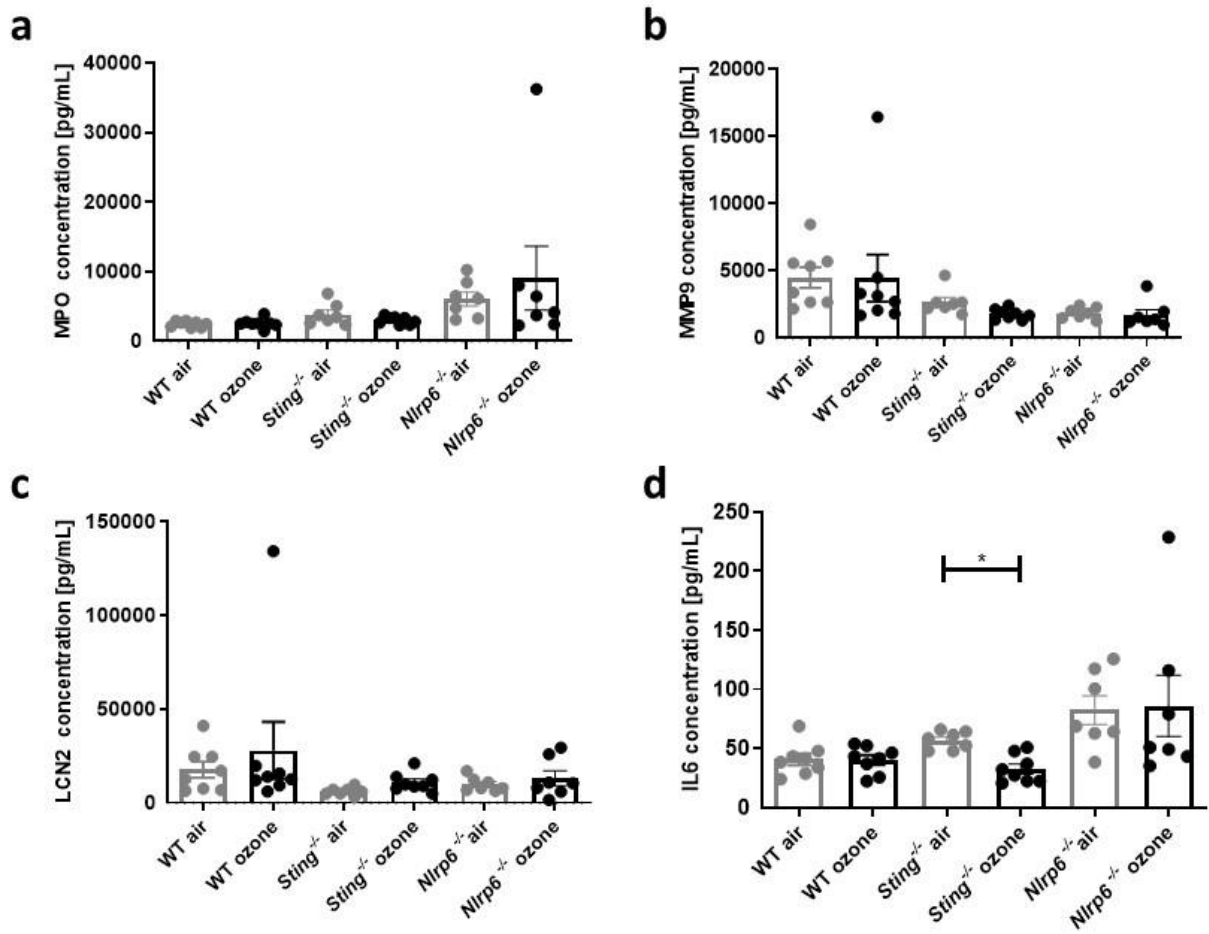*Figure 15*. MPO (a), LCN2 (b), MMP9 (c) and IL6 (d) concentration after chronic ozone exposure (0,5-1,5 ppm, 2 times per week, during 6 weeks) of wild-type (WT) and knock-out (*Sting*^{-/-}, *Nlrp6*^{-/-}) groups of mice. Data are represented as mean ± SEM. [***] P < 0.001, [**] P< 0.01, and [*] P< 0.05.

3.4. Chemical damage of the skin – cigarette smoke model

3.4.1. Histological analysis

Histological analysis of ear tissue sections from the mice that were subjected to cigarette smoke did not show any differences compared to their matching control groups (air groups). No inflammation or cellular infiltration was detected in neither cigarette smoke groups or genotypes according to histological examination. Also, no difference in the ear thickness was observed (Figure 16).
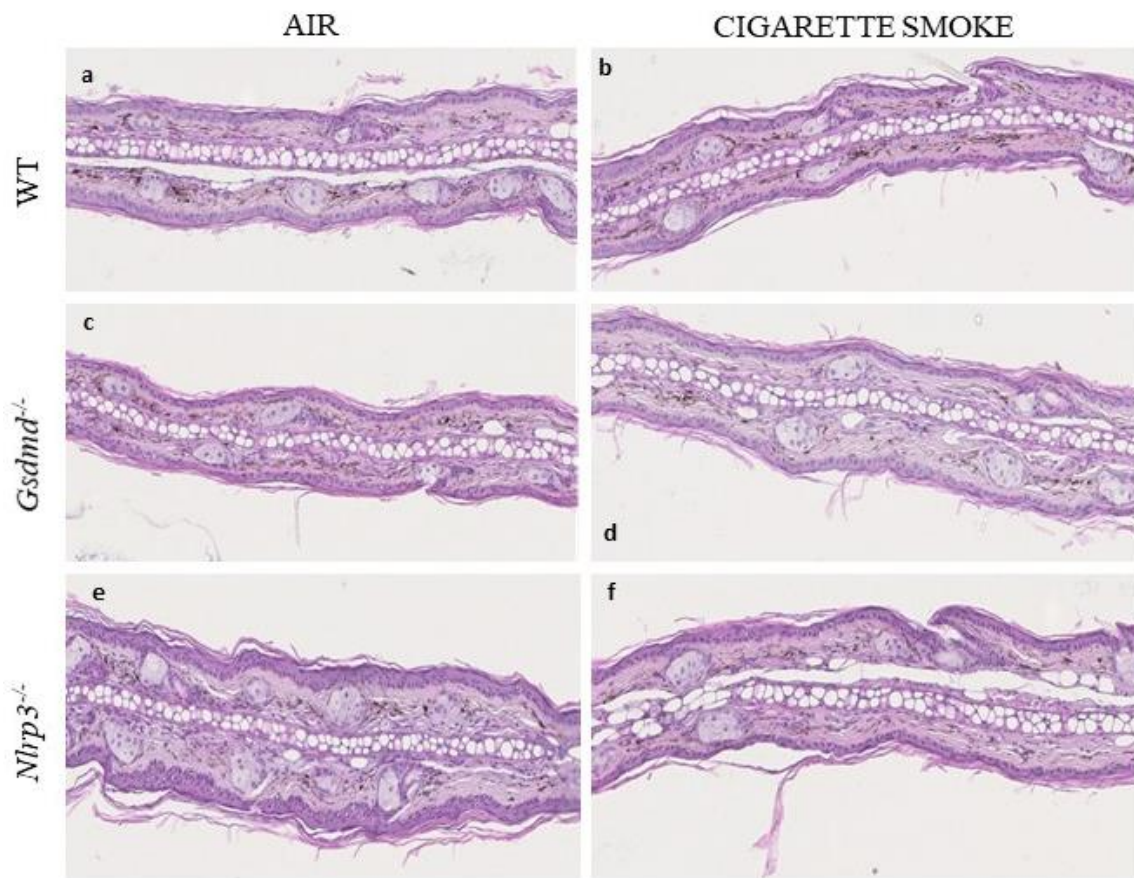
Figure 16. Histological evaluation and comparison of hematoxylin and eosin stained ears of control groups (air groups) of mice (a, c, e) and groups of mice which were subjected to cigarette smoke (CS, 12 cigarettes per day, during 4 days) (b, d, f) for both wild-type (WT) and knock-out mice (*Gsdmd*$^{-/-}$, *Nlrp3*$^{-/-}$). Photos were taken under 20x of magnification.

3.4.2. Protein dosage and infammatory mediator production

The concentration of all proteins was measured in order to detect whether inflammation occurred after exposure to cigarette smoke. No significant difference was observed in the

concentration of total proteins comparing all control (air groups) and cigarette smoke groups of both, wild-type (WT) and knock-out (*Gsdmd*$^{-/-}$, *Nlrp3*$^{-/-}$) mice (Figure 17).

Figure 17. Protein concentration after cigarette smoke (CS) exposure (12 cigarettes per day, during 4 days) of wild-type (WT) and knock-out (*Gsdmd*$^{-/-}$, *Nlrp3*$^{-/-}$) groups of mice. Data are represented as mean ± SEM. ***P < 0.001, **P< 0.01, and *P< 0.05.

Change in cytokine production after exposure to cigarette smoke was investigated by quantifying concentrations of four cytokines, MPO, LCN2, MMP9, and IL6. MPO production increased significantly in *Gsdmd*$^{-/-}$ cigarette smoke group of mice compared to the matching control group (*Gsdmd*$^{-/-}$ air) (Figure 18a). There was no significant difference in LCN2, MMP9, and IL6 production between cigarette smoke groups of mice and matching control groups (air groups) (Figure 18b-d).

Figure 18. MPO (a), LCN2 (b), MMP9 (c) and IL6 (d) concentration after cigarette smoke (CS) exposure (12 cigarettes per day, during 4 days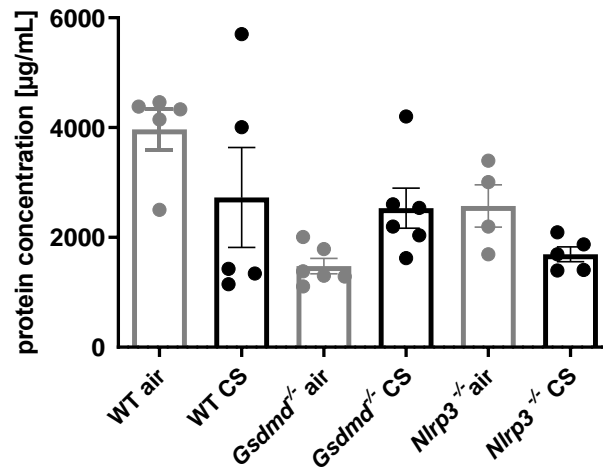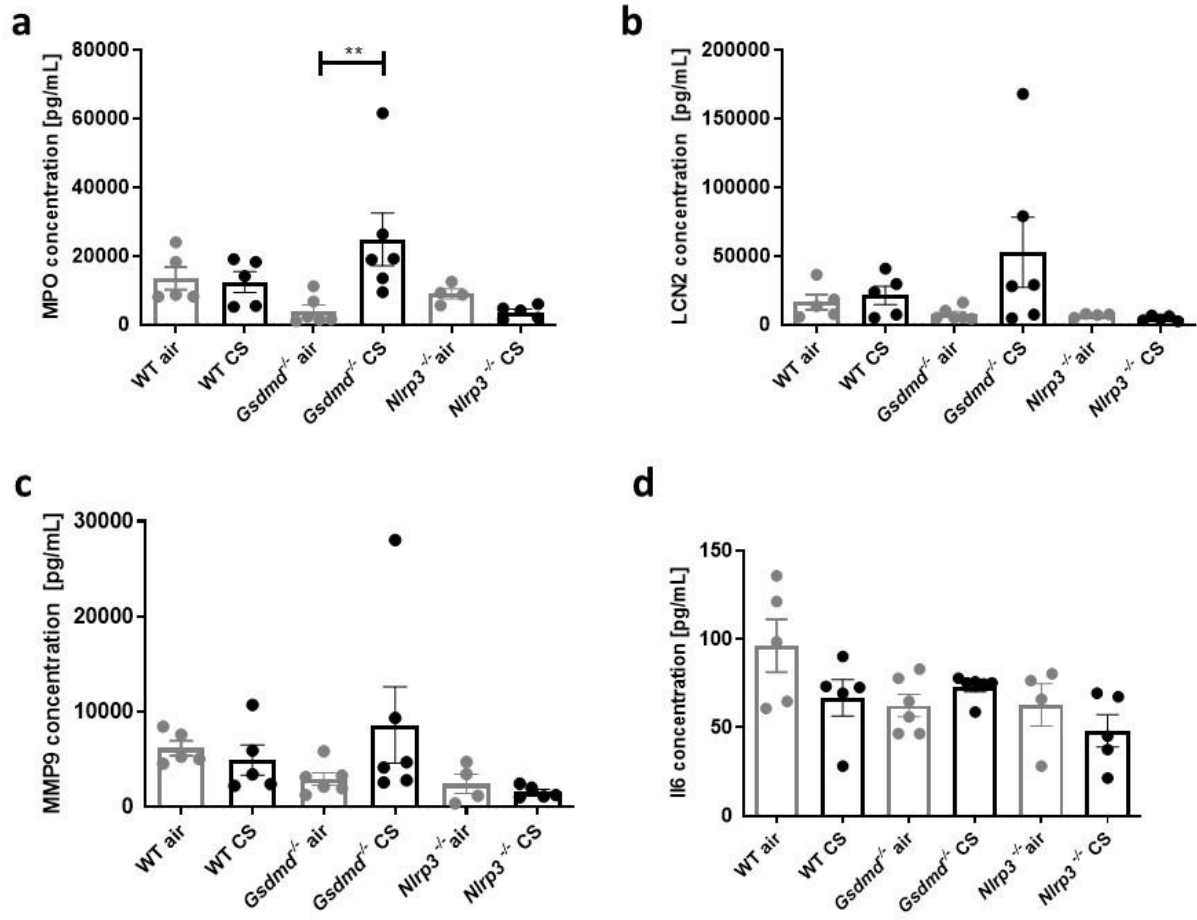) of wild-type (WT) and knock-out (*Gsdmd*^{-/-}, *Nlrp3*^{-/-}) groups of mice. Data are represented as mean ± SEM. [***] P < 0.001, [**] P< 0.01, and [*] P< 0.05.

4. DISCUSSION

Skin injuries are a major concern as the concentration of pollutants increases over time. Previous studies show severe inflammation in the lungs of mice exposed to cigarette smoke and ozone as well as inflammasome activation (Van der Vaart, 2004; Michaudel, 2016; Nascimento *et al.*, 2020). In this study, in order to examine inflammation, cellular infiltration, and the possible protective role of various DNA sensors after skin injury, mechanical and chemical models of skin injuries were established. Histological analysis and detection of inflammatory cytokines were performed for all research models.

4.1. Increased inflammatory response accompanying tape strip injury

According to histological analysis, it was noticed that the inflammation was present after mechanical damage of the skin with tape strip injury. It was shown that the thickness of the ear, as well as erythema and scaling of the skin, increased over time as the inflammation developed (Figure 5, 6). However, this trend was not observed in *Ifnar*$^{-/-}$ and partially *Sting*$^{-/-}$ TSI groups of mice which showed reduced inflammation. In those groups of mice, no significant difference in the ear thickness over time occurred compared to matching controls (Figure 5, 6).

The development of inflammation leads to an increase in temperature, and thus dilation of blood vessels, which is projected as redness/erythema of the skin (Flarer, 1955). Furthermore, epidermal desquamation is a highly regulated process of shedding of the corneocytes from the outermost layer of the stratum corneum. After mechanical damage of the skin, peeling skin occurs which refers to excessive visible surface desquamation (Has, 2018). Therefore, the absence of inflammation features in *Ifnar*$^{-/-}$ and partially in *Sting*$^{-/-}$ TSI mouse groups implies a possible protective effect of IFNAR and cGAS / STING pathway in skin injury.

Consequently, by analysing the production of proinflammatory cytokines, cellular infiltration was shown in WT, *Cgas*$^{-/-}$ and *Sting*$^{-/-}$ models which probably corresponded to neutrophil recruitment. Namely, cytokine production was enhanced in groups of mice on which tape strip injury was performed. However, decreased cytokine production was observed in *Ifnar*$^{-/-}$ TSI groups of mice suggesting a possible protective role of the interferon-α/β receptor (IFNAR) in skin injury.

By moving the upper layer of the epidermis, stratum corneum, inflammation occurs at the site of injury as well as infiltration of immune system cells which sense danger signals. Neutrophils are the first cells to appear at the site of injury and produce high concentrations of

proinflammatory cytokines to recruit innate effector cells as well as the other cells of the adaptive immune system (Richmond and Harris, 2014).

Therefore, our results indicate that TSI model of mechanical damage could be used in the investigation of mechanical skin injuries and that IFNAR may be a target for improved wound healing.

4.2. Mild inflammation after acute and chronic ozone exposure

Comparing both models, there was no difference in histological analyses between ear tissue sections taken from the mice that were exposed to acute or chronic ozone and their matching controls.

For the acute ozone model, a trend of possible neutrophil recruitment is detected, shown as an increase in the production of the cytokines. This trend was only observed for the wild-type and $Cgas^{-/-}$ groups of mice, but not in the $Sting^{-/-}$, $Ifnar^{-/-}$ and $Nlrp3^{-/-}$ groups of mice suggesting that for those groups, pathways were activated.

For the chronic ozone model, such results were shown only for the $Sting^{-/-}$ group of mice. Analysing the data, there is a possibility that STING was activated in the view of reduced IL6 production, but other parameters did not show a major effect.

Previous studies have shown that acute ozone exposure causes respiratory epithelial disruption with protein leak and neutrophil recruitment in the broncho-alveolar space, hence, leading to lung inflammation in the mice. Also, all these parameters are increased upon chronic ozone exposure, including collagen deposition (Michaudel *et al*., 2018). Furthermore, it was reported that ozone causes oxidative stress and inflammasome activation in the mouse lungs, thus releasing different cytokines such as IL1, MPO, and many others (Michaudel, 2016). However, such results were not fully obtained for the skin model, but slight inflammation and a possible protective role of STING, NLRP3, and IFNAR are noticeable. Although the mice were visibly sick, the skin proved to be very protective. In order to investigate if ozone is more destructive to the skin, the increment of the ozone concentrations to which mice are exposed, as well as the exposure time are needed. Still, further research and analysis are required to confirm those hypotheses.

4.3. Absence of inflammation after cigarette smoke exposure

According to histological examination and analyses of total protein concentration and cytokines, increased inflammation in the ear tissue sections from the mice which were exposed

to cigarette smoke was not detected. For the used exposure of the cigarette smoke, the parameters that we investigated are not conclusive whether cigarette smoke has an effect on inflammation.

However, previous studies indicate clear inflammation in the mouse lungs after cigarette smoke exposure. Increased production of cytokines BAFF, TNF-α, IL-6, MPO, and many others proved to be the biggest indicators of inflammation (Van der Vaart, 2004; Nascimento *et al*., 2020). Moreover, it was obtained that human skin of active and passive smokers has enhanced skin barrier damage, skin dryness, and wrinkles (Egawa *et al*., 1999; Ortiz and Grando, 2012). Considering this, it was hypothesized that such or a similar effect would appear on the skin, but in this study, no such outcome was observed suggesting that higher exposure time and dose of cigarette smoke are needed to cause inflammation.

5. CONCLUSIONS

In this study, mechanical (tape strip injury) and chemical (ozone and cigarette smoke) skin injury were investigated. By analysing the data, we concluded that mechanical skin damage is much more destructive than chemical-induced skin damage. However, higher doses and longer exposure of mice to ozone and cigarette smoke could have a more severe impact. We noticed a possible protective role of individual DNA sensors. IFNAR has been shown to participate in the DNA sensor pathway with the greatest protective role potential, followed by NLRP3 and STING. Namely, in order to show how these sensors act on inflammation and wound repair, additional research and analysis are needed.

6. REFERENCES

Bouwstra, J. and Honeywell-Nguyen, P. (2002) Skin structure and mode of action of vesicles. *Advanced Drug Delivery Reviews.* **54**: 41–55.

Di Dmizio J., Belkhodja C., Chenuet P., Fries A., Murray T., Marcos Mondéjar P., Demaria O., Conrad C., Homey B., Werner S., Speiser D. E., Ryffel B. and Gillet M. (2020) The commensal skin microbiota triggers type I IFN – dependent innate repair responses in injured skin. *Nature Immunology.* **21**: 1034–1045.

Drakaki E., Dessinioti C. and Antoniou C. V. (2014) Air pollution and the skin. *Frontiers in Environmental Science.* **2.**

Egawa M., Kohno Y., and Kumano Y. (1999) Oxidative effects of cigarette smoke on the human skin. *International journal of cosmetic science.* **21.2**: 83-98.

Ferrara F., Pambianchi E., Pecorelli A., Woodby B., Messano N., Therrien J.-P. and Valacchi, G. (2019) Redox regulation of cutaneous inflammasome by ozone exposure. *Free Radical Biology and Medicine.*

Flarer F (1955) The causes of inflammatory erythema. *Journal of Investigative Dermatology.* **24** (3): 201-209.

Has C. (2018) Peeling Skin Disorders: A Paradigm for Skin Desquamation. *Journal of Investigative Dermatology,* **138** (8): 1689-1691.

Hattori, Y., Kanbe, A., Ito, H., and Seishima, M. (2019) Activation of STING signaling accelerates skin wound healing. *Journal of Dermatological Science.*

Honari G., Andersen R. M. and Maibach H.I. (2017) Skin structure and function. In: *Senstive skin syndrome,* CRC Press. pp. 16-19.

Ivashkiv L. B. and Donlin L. T. (2014) Regulation of type I interferon responses. *Nat. Rev. Immunol.* **14:** 36–49.

Kim H. S., Noh S. U., Han Y. W., Kim K. M., Kang H., Kim H. O., and Park Y. M. (2009) Therapeutic Effects of Topical Application of Ozone on Acute Cutaneous Wound Healing. *Journal of Korean Medical Science.* **24** (3): 368.

Kisseleva T., Bhattacharya S., Braunstein J. and Schindler C. (2002). Signaling through the JAK/STAT pathway, recent advances and future challenges. *Gene.* **285** (1-2): 1–24.

Logan, J. A. (1985) Tropospheric ozone: Seasonal behavior, trends, and anthropogenic influence. *Journal of Geophysical Research: Atmospheres.* **90** (D6): 10463–10482.

Michaudel C., Couturier-Maillard A., Chenuet P., Maillet I., Mura C., Couillin, I., Gombault A., Quesniaux F. V., Huaux F. and Ryffel B. (2016). Inflammasome, IL-1 and inflammation in ozone-induced lung injury. *American journal of clinical and experimental immunology.* **5** (1): 33.

Michaudel C., Fauconnier L., Julé Y. and Ryffel, B. (2018). Functional and morphological differences of the lung upon acute and chronic ozone exposure in mice. *Scientific Reports.* **8** (1).

Nascimento M., Huot-Marchand S., Gombault A., Panek C., Bourinet M., Fanny M., Savigny F., Schneider P., Marc Le Bert, Ryffel B., Riteau N., Quesniaux F. V. and Couillin I. (2020) B-Cell Activating Factor Secreted by Neutrophils Is a Critical Player. *Lung Inflammation to Cigarette Smoke Exposure. Frontiers in Immunology.* **11.**

Ortiz A., and Grando S. A. (2012). Smoking and the skin. *International Journal of Dermatology,* **51**(3): 250–262.

Pestka S., Krause C. D., and Walter M. R. (2004). Interferons, interferon-like cytokines, and their receptors. *Immunological Reviews.* **202** (1), 8–32.

Richmond J. M. and Harris, J. E. (2014) Immunology and Skin in Health and Disease. *Cold Spring Harbor Perspectives in Medicine.* **4** (12).

Robert C. and Kupper T. S. (1999) Inflammatory Skin Diseases, T Cells, and Immune Surveillance. *New England Journal of Medicine.* **341** (24): 1817–1828.

Tschopp J. and Schroder K. (2010). NLRP3 inflammasome activation: the convergence of multiple signalling pathways on ROS production. *Nature Reviews Immunology.* **10** (3).

Van der Vaart H. (2004). Acute effects of cigarette smoke on inflammation and oxidative stress: a review. *Thorax.* **59** (8): 713–721.